Theoretical study of a dual harmonic system and its application to the CSNS/RCS *

YUAN Yao-Shuo(苑尧硕)   WANG Na(王娜)   XU Shou-Yan(许守彦)   YUAN Yue(袁月)   WANG Sheng(王生)[1)]

Dongguan Branch, Institute of High Energy Physics, Chinese Academy of Sciences, Dongguan 523803, China

Abstract: Dual harmonic systems have been widely used in high intensity proton synchrotrons to suppress the space charge effect, as well as reduce the beam loss. To investigate the longitudinal beam dynamics in a dual rf system, the potential well, the sub-buckets in the bunch and the multi-solutions of the phase equation are studied theoretically in this paper. Based on these theoretical studies, optimization of bunching factor and rf voltage waveform are made for the dual harmonic rf system in the upgrade phase of the China Spallation Neutron Source Rapid Cycling Synchrotron (CSNS/RCS). In the optimization process, the simulation with space charge effect is done using a newly developed code, C-SCSIM.

Key words: dual harmonic rf system, longitudinal beam simulation, rf voltage waveform, bunching factor

1   Introduction

The space charge effect is the principal cause of emittance growth and beam loss in high intensity accelerators. In high intensity synchrotrons, the space charge effect is the limit of the maximum number of particles that can be accumulated. The space charge induced tune shift is always used as a standard of space charge, and in a synchrotron, the relation between the bunching factor B_f and the tune shift $\Delta\nu$ is [1]

$$\Delta\nu = -\frac{r_\mathrm{p} n_\mathrm{t}}{2\pi\beta^2\gamma^3\epsilon B_\mathrm{f}}, \qquad (1)$$

where r_p is the classical radius of the proton, n_t is the bunch population, ϵ is the transverse emittance, and β and γ are the relativistic factors. To decrease the space charge tune shift, increasing the bunching factor by using a dual harmonic rf system is a common method in high intensity proton synchrotrons [2–5].

The China Spallation Neutron Source (CSNS) [6, 7] is a pulsed neutron source with beam power of 100 kW, which is currently under construction. Its accelerator consists of an 80 MeV H$^-$ linac and a 1.6 GeV proton Rapid Cycling Synchrotron (RCS). In a future upgrade, the beam power will upgrade to 500 kW. As an important way of depressing the space charge effect, a dual harmonic rf system will be employed in the RCS in the upgrade stage. In this paper, some important beam dynamics issues in the dual rf system, such as the potential well, the multi-solutions of the phase equation and

the sub-buckets in the bunches are studied theoretically. Based on these theoretical studies, optimizations of the bunching factor and rf voltage waveform are made for the dual harmonic rf system in the upgrade stage of the CSNS/RCS. In the optimization process, simulation with the space charge effect is done by using a newly developed code C-SCSIM [8]. The relation between bunching factor and rf voltage is studied and the corresponding beam distribution in the phase space is presented.

2   Theoretical study

2.1   The potential well

To obtain a concise formula for the potential well, coordinates $(\phi,\ P)$ are used [9]. Here, ϕ is the phase relative to the fundamental rf cavity and

$$P = -\frac{h\eta|\delta|}{\nu_\mathrm{s}}, \qquad (2)$$

where h is the ratio between the harmonic numbers in the fundamental rf system and higher harmonic rf system ($h=2$ for dual rf system), η is the phase slip factor, δ is the momentum deviation, and ν_s is the synchrotron tune at zero amplitude for the fundamental rf system. The Hamiltonian in this coordinate system can be written as

$$H(p) = \frac{1}{2}\nu_\mathrm{s}P^2 + U_1(\phi) + U_2(\phi), \qquad (3)$$

$$U_1(\phi)=\nu_s[\cos\phi_{1s}-\cos\phi+(\phi_{1s}-\phi)\sin\phi_{1s}], \quad (4)$$

$$U_2(\phi)=\frac{\nu_s r}{h}\{\cos\phi_{2s}-\cos[\phi_{2s}+h(\phi-\phi_{1s})]-h(\phi-\phi_{1s})\sin\phi_{2s}\}, \quad (5)$$

where U_1 and ϕ_{1s} are the potential energy and synchronous phase in the fundamental cavity, while U_2 and ϕ_{2s} are those for the second-harmonic cavity, and r is the ratio of the second-harmonic voltage and fundamental voltage, i.e. $r=-V_2/V_1$. The total voltage can be expressed as

$$V(\phi)=V_1\sin\phi+V_2\sin(2\phi-\phi_2), \quad (6)$$

where ϕ_2 is the rf phase angle of the second-harmonic cavity relative to the fundamental one,

$$\phi_2=2\phi_{1s}-\phi_{2s}. \quad (7)$$

Substituting Eq. (7) into Eq. (5), the potential energy in the dual harmonic rf system can be expressed as

$$U(\phi)=\nu_s[-\cos\phi-\phi\sin\phi_s+\frac{r}{2}\cos(2\phi-\phi_2)+r\phi\sin(2\phi_s-\phi_2)]. \quad (8)$$

2.2   The effect of r on the potential well

For simplicity, we assume ν_s equals 1. The curves of the function $U(\phi)$ in Eq. (8) are plotted in Fig. 1, which shows that the shape of the potential well changes as r varies from 0.4 to 0.8. From the figure we can see that when r becomes larger, the bottom of the potential well becomes higher.

In order to explain the results, we take the first-order derivative of the potential formula in Eq. (8):

$$\frac{\mathrm{d}U(\phi)}{\mathrm{d}\phi}=\nu_s[\sin\phi-\sin\phi_s-r\sin(2\phi-\phi_2)-r\sin(2\phi_s-\phi_2)] \quad (9)$$

which gives

$$\left.\frac{\mathrm{d}U(\phi)}{\mathrm{d}\phi}\right|_{\phi=\phi_s}\equiv 0. \quad (10)$$

Therefore, the slope at $\phi=\phi_s$ is equal to zero, and is independent of the value of ϕ_s and ϕ_2. Moreover, the second derivative is

$$\frac{\mathrm{d}^2U(\phi)}{\mathrm{d}\phi^2}=\cos\phi-2r\cos(2\phi-\phi_s). \quad (11)$$

Letting r equal 0.5, we have

$$\left.\frac{\mathrm{d}^2U(\phi)}{\mathrm{d}\phi^2}\right|_{\phi=\phi_s}\equiv 0, \quad (12)$$

which means the potential well is always flat at $\phi=\phi_s$.

2.3   Multi-solutions and two sub-buckets

If we assume $\nu_s=1$, $\phi_s=0$ and $\phi_2=0$, Eq. (8) can be simplified to

$$\frac{\mathrm{d}U(\phi)}{\mathrm{d}\phi}=\frac{\omega_0 eV_1}{2\pi\beta^2 E}[\sin\phi-r\sin(2\phi)]=0, \quad (13)$$

which gives,

$$2r\cos\phi-1=0. \quad (14)$$

The relation between r and ϕ in Eq. (14) are listed in Table 1. It can be seen that when $r>0.5$, Eq. (8) has two solutions, corresponding to the two minima of the potential well, as shown in Fig. 1(a), (b).

On the other hand, the total rf voltage in the dual harmonic system is

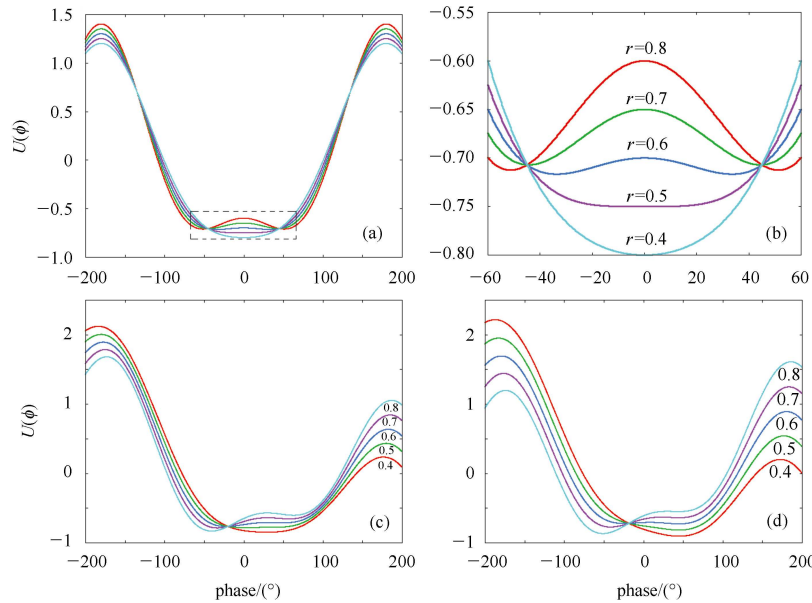$$V(\phi)=V_1[\sin\phi-r\sin(2\phi-\phi_2)]. \quad (15)$$

Fig. 1.   (color online) Variation of potential energy with different r. (a) $\phi_s=\phi_2=0$; (b) enlarged view of bottom part of (a); (c) $\phi_s=30°$, $\phi_2=30°$; (d) $\phi_s=45°$, $\phi_2=15°$.
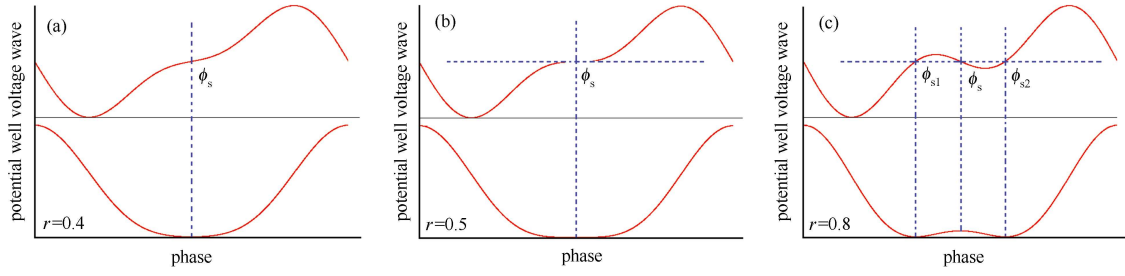
Fig. 2. (color online) Schematic drawing of the voltage wave and the potential at (a) r=0.4; (b) r=0.5 and (c) r=0.8.

Table 1. Relationship between r and ϕ.

r	$\phi/(°)$
0.4	nan
0.5	0
0.6	±33.6
0.7	±44.4
0.8	±51.3

Table 2. Main input parameters used in the simulation.

parameters	values
circumference/m	227.92
bending radius/m	8.021
repetition rate/Hz	25
harmonic number	2
chopping factor	0.5
injection turn	500
injection energy/MeV	250
extraction energy/GeV	1.6
number of protons (10^{13})	7.8
starting time at injection/ms	−0.3
macro-particle for injection	20000

In the accelerating process, the rf voltage should be

$$V(\phi)=\rho L \frac{\mathrm{d}B(t)}{\mathrm{d}t}, \qquad (16)$$

where ρ and L denote the bending radius and the circumstance of the ring respectively, and B is the magnetic field of the dipole. As shown in Fig. 2, when $r<0.5$, Eq. (16) has only one solution, i.e. the synchronous phase ϕ_s, but when $r>0.5$, there are three solutions: one is the synchronous phase ϕ_s, and the other two solutions are ϕ_s1 and ϕ_s2. When $r>0.5$, the voltage function is no longer monotonic.

In that case, ϕ_s1 and ϕ_s2 correspond to the two minima of the potential well. In this case, particles in the bucket can be divided into two parts by their energy deviation ΔE: those with small ΔE are trapped within the two "depressions" in the potential well, and can only oscillate within the range of the two sub-buckets, as marked by the square dots in Fig. 3; those with larger ΔE can extend to the whole bucket, as marked by the round dots. The "sub-buckets" plotted as a schematic drawing in Fig. 3, can be observed by beam simulation, as shown in Figs. 5–6.

2.4 Effects of ϕ_s and ϕ_2 on the potential well

Letting r=0.5, variation of the curve of the potential well with different ϕ_s and ϕ_2 is shown in Fig. 4.

To sum up, r affects the extent of the flatness in the bottom of the potential well, which is the reason for the formation of the sub-bucket in a bucket. The bottom is symmetrical about the line $\phi=\phi_\mathrm{s}$ when $\phi_\mathrm{s}=\phi_2=0$, and
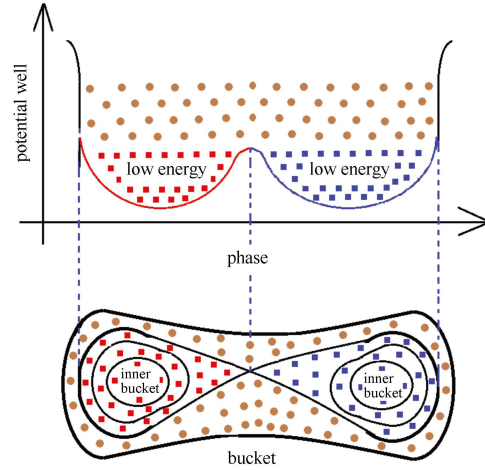

Fig. 3. (color online) Schematic drawing of particles with various ΔE in the potential well and in the two sub-buckets.

becomes uneven when either $\phi_\mathrm{s}\neq0$ or $\phi_2\neq0$. The uneven depends on the value of ϕ_s or ϕ_2.

3 Application to CSNS/RCS

3.1 Optimization of the bunching factor

In Section 2, we have obtained theoretically the formula for the potential well and how the four coefficients ϕ_s, ϕ_2, V_1 and V_2 influence the shape of the potential well. In fact, these parameters are not independent. Also, it is difficult to find an analytic solution for the bunching factor, which can often be considered as a crucial parameter in the dual harmonic system and taken as a key criterion in the rf voltage optimization process.
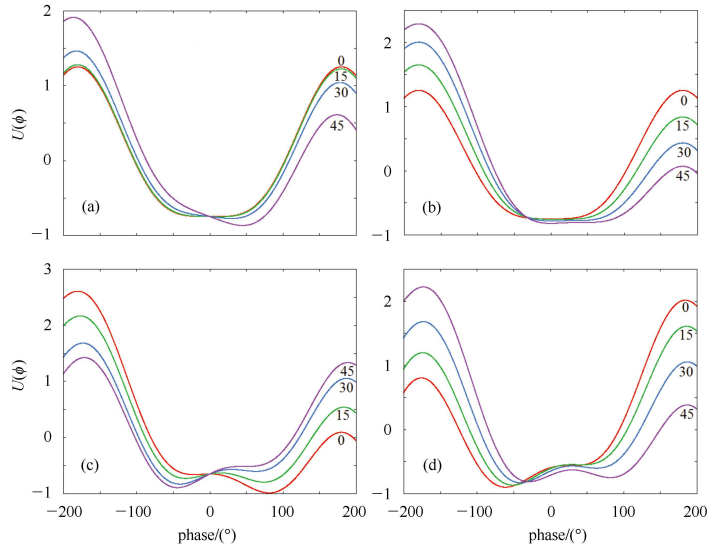
Fig. 4.   (color online) The curve of the potential well with $r=0.5$: (a) ϕ_s vs. U, with $\phi_2=0$; (b) ϕ_2 vs. U, with $\phi_s=0$; (c) ϕ_s vs U, with $\phi_2=30°$; (d) ϕ_2 vs. U, with $\phi_s=30°$.
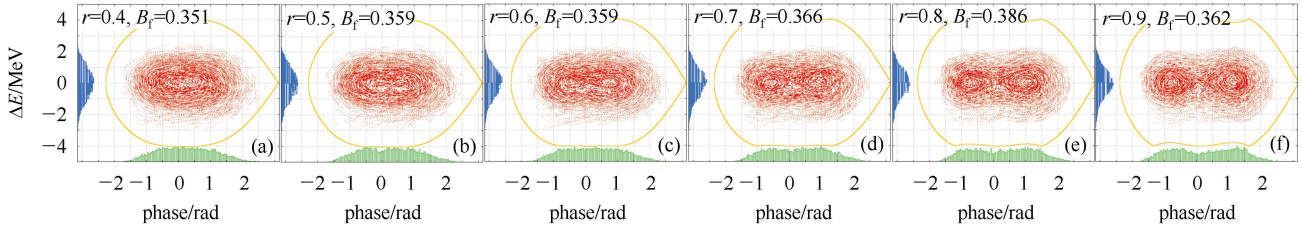

Fig. 5.   (color online) Particle distribution with different r at the end of the injection (500th turn, $\phi_s=8.2°$, $\phi_2=14.0°$, $V_1=77.8$ kV).
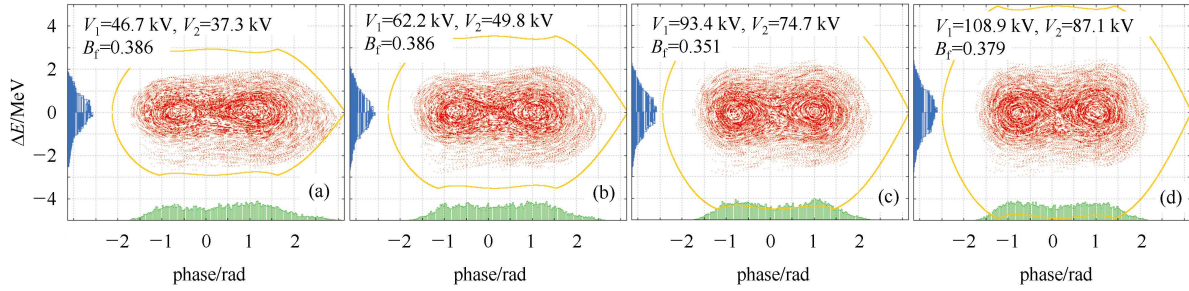

Fig. 6.   (color online) Particle distributions with different V_1 and V_2 at the end of the injection process.

In the upgrade stage of CSNS/RCS, the dual harmonic system will be employed to achieve uniform longitudinal beam distribution (i.e. a flat potential well) and much larger bunching factor. Early studies have been performed for the upgrade case of 200 kW beam power [10]. Here, by using the simulation code C-SCSIM, the relation between the potential well and the bunching factor for the case of 500 kW beam power is investigated. Table 2 lists the input parameters used in the simulation.

The simulation was performed in two steps. First, during 0–2 ms in an accelerating process, the value of r

$(r=-V_2/V_1)$ was scanned from 0.4 to 0.9 by increasing V_2 while keeping V_1 as a constant in each time point, as listed in Table 3. The simulation results are shown in Fig. 5. One can see that as r increases, both the top and the bottom of the bucket shrink while the bunching factor increases at first and then decreases. Moreover, when $r >0.5$, the bunch divides into two sub-buckets, and they tend to become more and more "clear" as r increases. We can also observe that when r equals 0.5, the bucket becomes flat, but the bunching factor is not at its maximum.

For the second step, V_1 and V_2 were changed, but r was kept constant. Letting the values of V_1 and V_2 used in the Fig. 5(f) be a reference, the values were multiplied by factors of 0.6, 0.8, 1.2 and 1.4. The simulation results

Table 3.   Fundamental voltage waveform used in step 1 of the simulation.

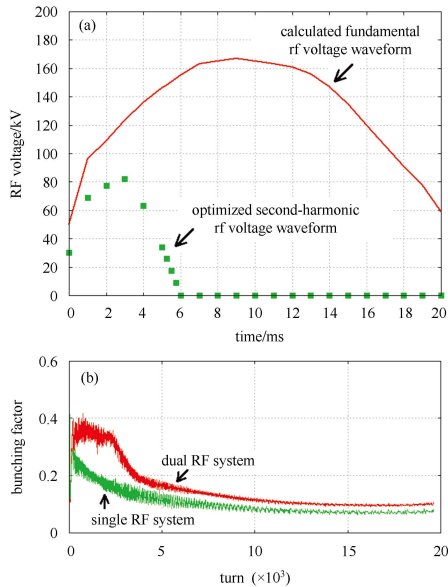| time/ms	fundamental voltage/kV
0	50
1	95
2	110

Fig. 7.   (color online) (a) Optimized voltage waveform; (b) Comparison of the bunching factor in dual and single rf systems.

are shown in Fig. 6, from which we can observe that as V_1 and V_2 increase, the area of the bucket is enlarged but the area of the bunch and the bunching factor does not change much compared with the case in Fig. 5.

3.2   Optimization of rf voltage waveform

Based on the properties of the bunching factor obtained above, the voltage waveform can be optimized with an iteration method using the code C-SCSIM. Generally, the optimization procedure consists of two steps.

At first, the fundamental rf voltage is calculated using the iteration method [3]. Secondly, the second rf voltage waveform is optimized according to the beam distribution and the bunching factor calculated by using the code.
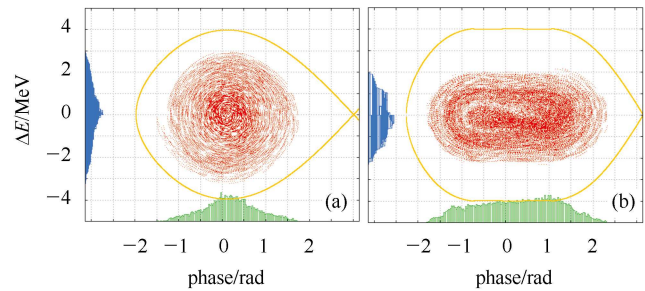

Fig. 8.   (color online) Comparison of the beam distribution at the 500th turn for upgrade phase with (a) single rf system and (b) dual rf system.

The calculated fundamental rf voltage waveform and the optimized second-harmonic rf voltage waveform are shown in Fig. 7(a). Figure 8 gives the particle distribution at the 500th turn for the upgraded CSNS/RCS, using only the calculated fundamental rf voltage waveform and the dual harmonic system, respectively. From Fig. 8(b) and Fig. 7(b) it can be seen that under the optimized second-harmonic rf voltage waveform, the particle distribution becomes flat and the bunching factor has increased significantly.

4   Summary

Beam dynamics for a dual harmonic rf system has been investigated by theoretical analysis. The influence of the rf voltage, the relative phase ϕ_2 and the synchronous phase ϕ_s on the shape of the potential well have been introduced. The bunching factor and the formation and characteristics of the sub-buckets in the bunches have been illustrated. These theoretical results are applied to the optimization design of a dual harmonic rf system for the future upgrade of CSNS/RCS, and the results are important for the dual rf system design for the upgrade stage.

References

1 Laslett L J. Proc. 1963 Summer Sch. BNL, 1963. 324–326
2 Baillod J M, Magnani L, Nassibian G et al. IEEE Trans. Nucl. Sci., 1983, **729**: 3499–3501
3 Brennan J M, Roser T. Proc. of PAC1999. New York, 1999. 614–616
4 Middendorf M E, Brumwell F R, Dooling J C et al. Proc. of PAC2007. Albuquerque, New Mexico, 2007. 2233–2235
5 Yamamoto M et al. Nucl. Instrum. Methods A, 2010, **621**: 15–32
6 CSNS Project Team. China Spallation Neutron Source Feasibility Reaearch Report. Institute of High Energy Physics and Institute of Physics, Chinese Academy of Sciences, 2009 (in Chinese)
7 WEI J et al. Chin. Phys. C, 2009, **33**: 1033–1042
8 YUAN Y S et al. Nucl. Instrum Methods A, 2013, **729**: 864–869
9 Lee S Y. Accelerator Physics, Singapore. World Scientific, 2004. 327–334
10 CHEN J F et al. Chinese Physics C, 2010, **34**: 1643–1648